Olefin Production by Catalytic Transformation of Crude Bio-Oil in a Two-Step Process

ARTICLE *in* INDUSTRIAL & ENGINEERING CHEMISTRY RESEARCH · NOVEMBER 2009

Impact Factor: 2.59 · DOI: 10.1021/ie901204n

Olefin Production by Catalytic Transformation of Crude Bio-Oil in a Two-Step Process

Ana G. Gayubo,* Beatriz Valle, Andrés T. Aguayo, Martin Olazar, and Javier Bilbao

Chemical Engineering Department, University of the Basque Country, P. O. Box 644, 48080, Bilbao, Spain

The valorization of crude bio-oil by catalytic transformation into hydrocarbons has been carried out in an online two-step (thermal-catalytic) process. The deposition of pyrolytic lignin, formed by polymerization of biomass-derived products, is enhanced in the thermal step. Volatiles are processed in a fluidized bed reactor with a catalyst that is hydrothermally stable and selective for olefin production, which has been based on a HZSM-5 zeolite. A study has been made of the effect of operating conditions (methanol content in the feed of bio-oil/methanol, temperature, space time, and time on stream) on bio-oil conversion, product lump yields and the selectivity of each individual C_2-C_4 olefin. These conditions also have a significant effect on deactivation, which is attributed to coke deposited on the catalyst. The TPO curves of coke combustion identify two fractions: one of thermal origin (pyrolytic lignin) and the other of catalytic origin, whose formation depends on the concentration of oxygenates in the reaction medium. A feed with 50 wt % of methanol, at 500 °C, with space time of 0.371 (g of catalyst) h (g of methanol)$^{-1}$ allows a 94 wt % conversion of the bio-oil in the feed, with a selectivity of C_2-C_4 olefins of 48 wt % (50 wt % is propene) and low yields of CO and CO_2 (its formation is attenuated by cofeeding methanol).

1. Introduction

The bio-oil obtained by flash pyrolysis of lignocellulosic biomass has good prospects to partially replace petroleum as a raw material, contributing effectively to reducing CO_2 emissions.[1,2] Flash pyrolysis produces bio-oil yields in the 60−75 wt % range (between 450 and 550 °C and depending on biomass composition and humidity), with char yield of 15−25 wt % and gas yield of 10−20 wt %.[3] This high yield of bio-oil can be achieved by processing the geographically dispersed biomass sources with small-scale units, where the energy required for pyrolysis can be supplied by the partial combustion of gas and char. The bio-oil could be stored and transported to refinery units (biorefinery), which are provided with the equipment and bench scale required to obtain fuels, synthesis materials (such as olefins and BTX), and hydrogen.[4−6] This strategy has better prospects for large-scale biomass valorization than the use of catalysts in situ in the pyrolysis reactor[7,8] and for the online processing of pyrolysis volatiles.[9,10]

Bio-oil is a polar and hydrophilic brown liquid made up of products from the depolymerization and fragmentation of cellulose, hemicellulose, and lignin, with a water content of around 25 wt % and an oxygen content of 45−50 wt %. Over 300 components have been identified by GC-MS (acids, alcohols, aldehydes, esters, ketones, phenols, guaiacols, syringols, sugars, furans, alkenes, aromatics, nitrogen compounds, and a variety of oxygen compounds).[11−14]

The viability of catalytic processes for the valorization of crude bio-oil is curtailed by the deposition of carbonaceous material (pyrolytic lignin) on the catalyst, which is formed by the condensation of the products from biomass lignin pyrolysis. Consequently, research on the catalytic transformation of bio-oil is almost limited to the study of either pure components of bio-oil or to the aqueous fraction (with a lower content of phenol derivatives and obtained after the separation into two phases of the crude bio-oil, by adding water up to 75 wt %). The pathways for the catalytic valorization of pure oxygenates and the bio-oil aqueous fraction that have deserved more attention are deoxygenation-cracking for obtaining hydrocarbons,[15,16] and steam reforming for obtaining hydrogen.[17−19]

In addition to the problem of the unavoidable deposition of pyrolytic lignin, crude bio-oil is highly unstable during storage. This instability is avoided by adding 10 wt % of methanol.[20,21] A previous study revealed that this addition of methanol contributes to reducing the deposition of pyrolytic lignin in the catalytic transformation of bio-oil, and this deposition is gradually reduced by increasing the methanol content in the bio-oil/methanol feed to 50 wt %.[22] Furthermore, controlling the deposition of pyrolytic lignin in a specific step of thermal treatment prior to the catalytic reactor minimized deposition on the catalyst and thereby attenuates deactivation.[23]

In this work we have applied these two strategies together: cofeeding methanol along with crude bio-oil into a two-step (thermal-catalytic) reaction system, for obtaining C_2-C_4 olefins selectively. The use of HZSM-5 catalysts is advisible for this purpose, based on their good behavior for obtaining olefins from bio-oil containing pure compounds and, in general, for the treatment of oxygenates.[24,25]

2. Experimental Section

2.1. Bio-Oil Production and Composition. The bio-oil has been obtained at 450 °C using a N_2 stream in a pilot plant provided with a conical spouted bed reactor,[7,11,26] by feeding pine (*Pinus insignis* (*P. insignis*)) sawdust with a particle size between 0.8 and 2 mm. The bio-oil used in this study corresponds to a 75−76 wt % fraction of the whole bio-oil, given that in order to attain product reproducibility the bio-oil studied is that collected in the condenser and in the ice−water trap, whereas that retained in the coalescence filter has been discarded. The composition of the crude bio-oil (Table 1) was determined by GC/MS analysis in a GC/MS (Shimadzu QP2010S) device provided with a TBR-1MS column. The values of the error intervals included in Table 1 for the percentages of each family of components have been calculated by analyzing five samples obtained under the same conditions.

* To whom correspondence should be addressed. Tel.: +34 946 015459. Fax: +34 946 013 500. E-mail: anaguadalupe.gayubo@ehu.es.

10.1021/ie901204n CCC: $40.75
Published on Web 11/18/2009

Table 1. Component Families in the Crude Bio-Oil

component	wt %	component	wt %
acetic acid	15.3 ± 0.2	phenols	8.2 ± 0.7
acetone	5.3 ± 0.1	alcohols	11.6 ± 0.3
other ketones	21.8 ± 0.3	ethers	0.9 ± 0.1
other acids and esters	10.8 ± 0.5	levoglucosan	3.9 ± 0.4
hydroxyacetaldehyde	10.6 ± 0.2	others	1.3 ± 0.1
other aldehydes	8.7 ± 0.2	unidentified	1.6 ± 0.6

Product identification has been carried out by means of the NIST 147 library, and the correction factors for the chromatographic analysis have been determined by using 18 pattern mixtures containing the main components. Water content (48 wt % in the crude bio-oil) has been measured by gas chromatography (Agilent Micro GC 3000).

2.2. Reaction Equipment and Product Analysis. The thermal and catalytic cracking of bio-oil is carried out online in two separate units, which have been previously described in detail.[23] In the first unit (cylindrical tube made of S-316 stainless steel with an internal diameter of 5/8 in.), bio-oil is cooled with water at the inlet to avoid the condensation of pyrolytic lignin, which deposits on a bed of glass spheres, at 400 °C. In the second unit, the catalytic transformation of volatile compounds leaving the first unit is carried out. It is a fluidized bed reactor (inside a vertical cylindrical tube made of S-316 stainless steel with an internal diameter of 20 mm and a total length of 465 mm) which is located within a ceramic chamber heated by an electrical resistance. The catalyst bed is placed on a porous plate (at 285 mm from the reactor base).

The online analysis of the products is carried out every 5 min, with the samples being sent to a gas chromatograph (Agilent Micro GC 3000) provided with four modules for the analysis of the following: (1) permanent gases (O_2, N_2, H_2, CO, and CH_4); (2) oxygenates (MeOH, dimethyl ether, and CO_2), light olefins (C_2-C_3), and water; (3) C_2-C_6 hydrocarbons; (4) C_6-C_{12} hydrocarbons and oxygenate compounds. The volatile compounds that do not reach the analysis equipment are cooled in a Peltier condenser (0 °C), from which two streams leave (1) incondensable compounds that leave the reaction equipment through the outlet for gases and (2) the liquid fraction that is collected in a vessel placed on a digital balance (Electronic Balances EK-600H). Data gathering and processing are carried out by means of the software Soprane (Version 2.4.b).

2.3. Catalyst. The catalyst is prepared from HZSM-5 zeolite (with a SiO_2/Al_2O_3 ratio of 80). The zeolite is agglomerated (by wet extrusion) with bentonite (Exaloid), and using alumina (Prolabo) calcined at 1000 °C as inert charge. The proportion of each component in the catalyst is as follows: 25 wt % zeolite, 45 wt % bentonite, and 30 wt % alumina. The extrudates are dried at room temperature for 24 h. The particles are then ground and sieved to a size between 0.15 and 0.25 mm, dried at 110 °C for 24 h, and calcined at 575 °C for 2 h.

The physical properties (S_{BET}, 258 $m^2\ g^{-1}$; V_p, 0.58 $cm^3\ g^{-1}$; pore volume distribution, 6.6% for $d_p < 20$ Å, 37.1% for d_p between 20 and 500 Å, and 56.3% for $d_p > 500$ Å) have been determined by N_2 adsorption−desorption (Micromeritics ASAP 2010) and Hg porosimetry (Micromeritics Autopore 9220).

Total acidity (0.41 (mmol of NH_3) (g of zeolite)$^{-1}$) and acid strength distribution (uniform acidity with an average value of 130 kJ (mol of NH_3)$^{-1}$) have been determined by measuring the differential adsorption of NH_3 at 150 °C. Subsequently, TPD (temperature programmed desorption) of adsorbed NH_3 has been carried out following a ramp of 5 °C min^{-1} up to 550 °C, which shows a broad peak between 250 and 350 °C. The equipment used is a thermobalance (TA Instruments SDT 2960) online with a mass spectrometer (Balzers Instruments Thermostar).[27,28] The Brönsted/Lewis sites ratio has been determined by FTIR analysis (Nicolet 6700 provided with a Specac catalytic chamber) from the ratio between the adsorption bands intensity at 1545 and 1450 cm^{-1} for pyridine adsorbed at 150, 250, and 350 °C. The values obtained for these ratios are 0.95, 1.96, and 2.82, respectively.

The coke deposited on the catalyst has been studied by combustion with air in the TG/MS arrangement described above. A protocol has been followed in order to render the results reproducible.[29]

3. Results

3.1. Effect of Methanol Cofeeding. Figure 1 shows the results of the evolution with time on stream of product yields and oxygenate concentration at the reactor outlet. Each graph corresponds to a feed with different methanol content. The concentration of each lump of products, X_i, has been measured as the mass fraction by mass unit of total components in the reaction medium, excluding water. The products are grouped into the following: CH_4, CO + CO_2, aromatics, C_2-C_4 olefins, C_2-C_4 paraffins, and nonaromatic C_{5+}. Dimethyl ether (DME) is almost in thermodynamic equilibrium with methanol right from the reactor entrance, so it has been considered a reactant. Product yields (Y_i) were calculated by mass unit of organic compounds (oxygenates) fed into the reactor:

$$Y_i = \frac{\text{mass flow rate of lump } i \text{ at the reactor outlet}}{\text{mass flow rate of oxygenates fed into the reactor}} \quad (1)$$

The experimental results for the mass fraction of each lump in the product stream used for calculating the yields are the average of three runs repeated under the same conditions, whose maximum errors are as follows: aromatics, 1.2%; C_2-C_4 olefins, 1.0%; C_2-C_4 paraffins, 6.4%; nonaromatic C_{5+}, 1.7%; CO + CO_2, 2.1%.

The mass flow rate of oxygenates fed into the reactor was calculated by subtracting the amount of pyrolytic lignin deposited in the thermal treatment unit, which has been determined by runs of different duration, from the mass flow of oxygenates fed into the two-step (thermal + catalytic) system.

The results in Figure 1 confirm that high yields of hydrocarbons are obtained at 450 °C and that methanol in the feed attenuates catalyst deactivation, which is very fast when only crude bio-oil is in the feed (Figure 1a). This effect is known and attributed to an increase in the H/C ratio in the feed when methanol is cofed.[30]

It is also noteworthy that increasing the methanol content in the feed decreases the yield of CO and CO_2 at a higher rate than that corresponding to the decrease in the bio-oil content of in the feed. This effect is relevant because the formation of CO and CO_2 (by decarbonylation and decarboxylation of components) is one of the main drawbacks facing biomass derivative valorization, although as shown in Figure 1f the formation of CO and CO_2 is negligible in the catalytic transformation of methanol at 450 °C.

The conversion of bio-oil at zero time on stream has been estimated in the mixtures studied (Figure 2), being calculated from the bio-oil mass flow rates at the fluidized bed reactor inlet, $(m_{\text{bio-oil}})_i$, and outlet $(m_{\text{bio-oil}})_o$:

$$(X_{\text{bio-oil}})_{t=0} = \left[\frac{(m_{\text{bio-oil}})_i - (m_{\text{bio-oil}})_o}{(m_{\text{bio-oil}})_i}\right]_{t=0} \quad (2)$$

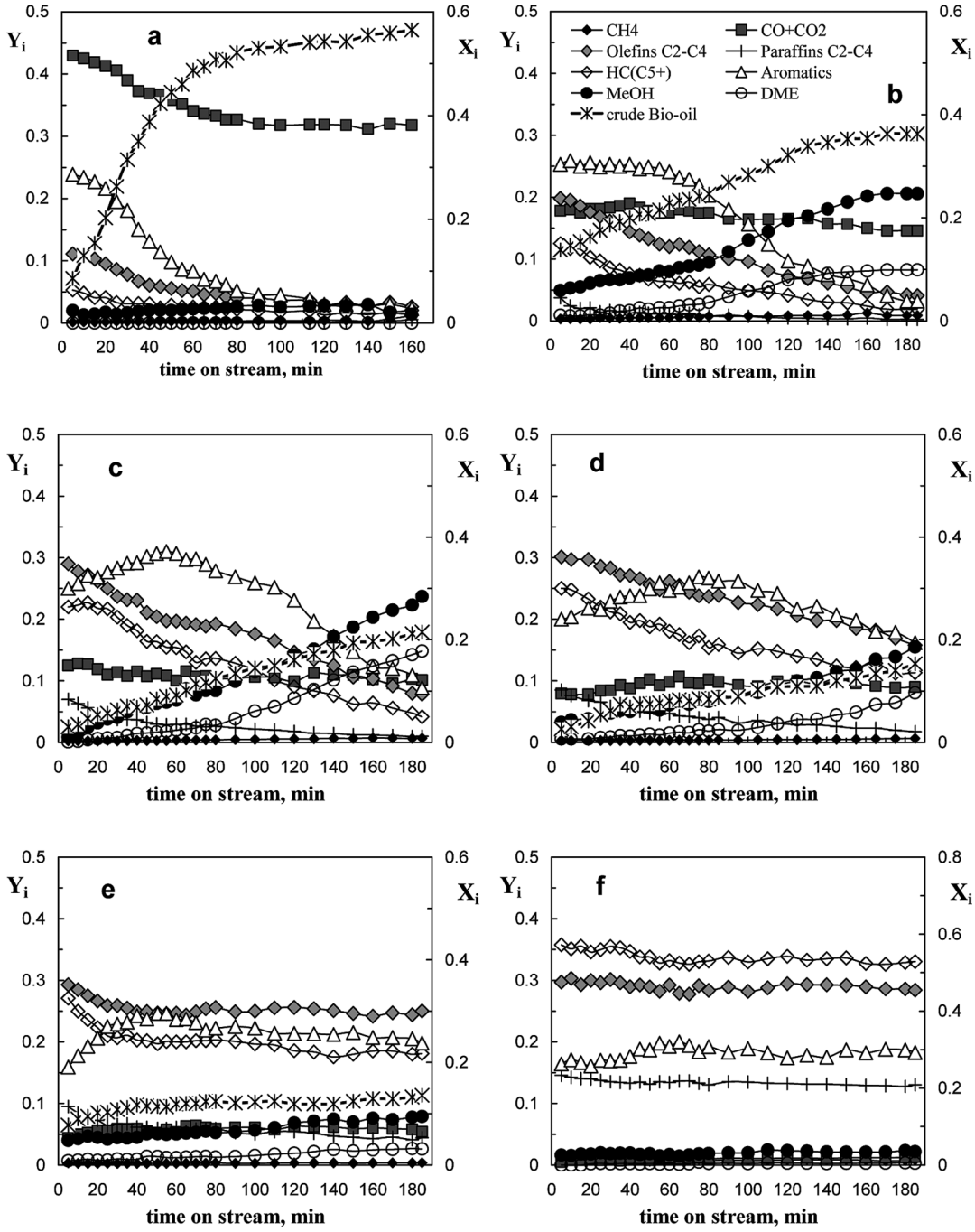

Figure 1. Effect of methanol content in the feed (bio-oil/methanol) on the evolution with time on stream of product yields and oxygenate concentration at the reactor outlet. Operating conditions: 450 °C; space time, 0.371 (g of catalyst) h (g of oxygenates)$^{-1}$: (a) feed, crude bio-oil; (b) bio-oil/methanol, 4:1 mass ratio; (c) bio-oil/methanol, 3:2 mass ratio; (d) bio-oil/methanol, 1:1 mass ratio; (e) bio-oil/methanol, 2:3 mass ratio; (f) methanol.

It should also be noted that the conversion of methanol fed in the mixtures is complete under the conditions studied. The results in Figure 2 show the existence of a slight peak in bio-oil conversion at zero time on stream (approximately 93 wt %) for 40 wt % methanol in the feed. In addition to the interest of this high conversion of bio-oil, the synergistic effect of methanol in the feed is relevant, being attributable to the reactivity of the light olefins formed from methanol. The presence of these olefins in the reaction medium presumably activates the steps for the formation of active intermediates after the adsorption of bio-oil oxygenates on the catalyst acid sites. The formation mechanisms are presumably similar to those for the *carbon pool*, which are well-established for the initial stages of methanol transformation into hydrocarbons.[31−33] The results confirm that a high content of methanol may cause the saturation of acid sites, on which methanol is adsorbed competitively with bio-oil oxygenates.

Methanol content in the feed also has a significant effect on product distribution and on their evolution with time on stream (Figure 1). Figure 2 also shows the effect of methanol content in the feed on product lump selectivity at zero time on stream. The selectivity of each *i* lump has been calculated on the basis of the yields of hydrocarbon products (without considering the yield of CO and CO_2).

$$(S_i)_{t=0} = \left[\frac{Y_i}{\sum_{\mathrm{HC}} Y_i}\right]_{t=0} \tag{3}$$

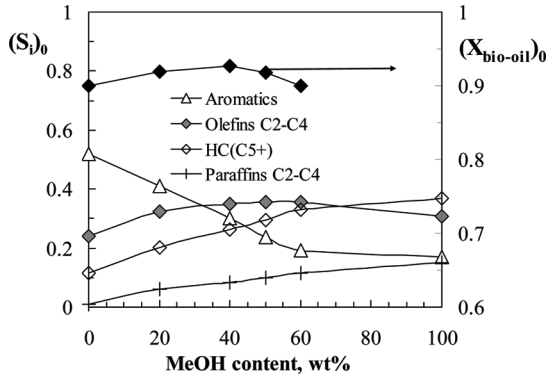

Figure 2. Effect of methanol content in the feed on bio-oil conversion and on the selectivity of hydrocarbon product lumps at zero time on stream. Operating conditions: 450 °C; space time, 0.371 (g of catalyst) h (g of oxygenates)$^{-1}$.

Figure 2 shows that olefin selectivity peaks at 50−60 wt % of methanol. It should be noted that this content also corresponds to the minimum yield of pyrolytic lignin deposited in the thermal step of the two-step process.[22] Aromatics selectivity decreases when methanol content in the feed is increased, whereas the selectivity of light paraffins and C_{5+} hydrocarbons increases significantly with methanol content.

The results in Figure 3 allow carrying out a detailed analysis of the effect of methanol content in the bio-oil/methanol feed on the evolution with time on stream of each C_2-C_4 olefin selectivity. Each graph corresponds to a feed composition. Selectivity, S_i', is different from that defined in eq 3, since it is based on the total yield of all products (including CO and CO_2).

By increasing the methanol content in the feed, the selectivity of C_2-C_4 olefins increases with the aforementioned peak at zero time on stream for a 50 wt % of methanol in the feed (Figure 3d). However, for a methanol content above 60 wt %, catalyst deactivation does not affect the selectivity of olefins (Figure 3e). It is noteworthy that propene is the predominant olefin, which makes the process more interesting since it is commercially the most valuable olefin, with a constant yield with time on stream of approximately 17 wt % for 60 wt % methanol in the feed (Figure 3e). Furthermore, an increase in methanol content in the feed leads to a decrease in ethene fraction and an increase in butanes fraction.

Figure 4 shows the TPO curves obtained in the combustion of coke deposited on the catalyst after reactions with different methanol contents in the feed. In the TPO curve corresponding to the transformation of pure methanol only one coke, of catalytic origin, is identified, peaking at 530 °C. However, in the curve for the catalyst deactivated by feeding crude bio-oil, a prior wider peak is observed, with a maximum at around 450 °C. These results, with a broad peak or multiple peaks, show the heterogeneous nature of the coke formed when bio-oil/methanol mixtures are fed.[29] TPO curve deconvolution allows identifying and quantifying two fractions,[22,23] whose contents, together with the total coke content, are shown in Table 2. The maximum relative error of these results is 5%.

These results are explained by the different origin of the two coke fractions. The coke fraction with a C_{c1} content, corresponding to the first peak in Figure 4, is of thermal origin and corresponds to the pyrolytic lignin, which is the same material as that deposited in the first step and also deposited on the catalyst. It is generated by the polymerization of bio-oil components derived from biomass lignin pyrolysis. The fact that it also deposits on the catalyst is because deposition in the thermal step is not totally efficient and, although the fraction deposited on the catalyst is small, it can significantly contribute to its deactivation. The fact that it burns easily is explained by its location on the outside of the catalyst particles and on the macropores generated between the HZSM-5 zeolite crystals and bentonite and alumina crystals. It should be noted that the deposition of pyrolytic lignin on the catalyst has been greatly attenuated in the two-step process, and when the crude bio-oil is fed directly into the catalytic bed, it causes rapid deactivation.[22]

The coke fraction with a C_{c2} content corresponds to the coke of catalytic origin, formed from hydrocarbon components in the reaction medium, by the well-known mechanisms of oligomerization, cyclization, aromatization, and condensation.[34,35] The catalytic coke in the transformation of methanol into hydrocarbons is reported to be generated by the condensation of polymethylarene intermediates toward polyaromatic structures in the formation of light olefins. The formation of these intermediates is enhanced by the concentration of oxygenates and olefins in the reaction medium.[36] Among the bio-oil oxygenated components, aldehydes, oxyphenols, and furfural stand out because of their capability for coke formation.[37]

The results in Figure 4 and Table 2 show that the major coke component is of catalytic origin, which is expected to make a more significant contribution to catalyst deactivation because it directly blocks the acid sites. Its location inside the crystals of HZSM-5 zeolite confirms that its combustion requires a higher temperature than thermal coke (Figure 4), which is a known fact in the combustion of coke on microporous catalysts.[29] In view of the values of coke content (Table 2), methanol in the feed efficiently contributes to reducing the catalytic coke content and even more so the deposition of thermal coke (pyrolytic lignin).

3.2. Effect of Temperature. Figure 5 shows the results of the evolution of product yields and mass fraction of oxygenates at the reactor outlet with time on stream. Each graph corresponds to a temperature. In view of the satisfactory results, the study has been carried out with the mixture of 50 wt % bio-oil/methanol. The results show a pronounced increase in hydrocarbon yields at zero time on stream when temperature is increased in the range 400−500 °C, which is due to the increase in methanol and bio-oil oxygenate conversion (Figure 6).

Figure 6 also shows the effect of temperature on product lump selectivities at zero time on stream. A steady increase is noted in C_2-C_4 olefin selectivity as temperature is increased, which is to be expected as olefins are products formed by higher hydrocarbon cracking reactions, which are enhanced by temperature. This is a well-known result in the transformation of methanol on HZSM-5 zeolite catalysts, in which light olefins are end products of oligomerization-cracking reactions above 400 °C. HZSM-5 zeolites also show this high selectivity of olefins in the cracking of petroleum fractions above 500 °C, and therefore they are used as additives in FCC catalysts.[38]

The selectivity of C_{5+} hydrocarbons does not change with temperature, whereas the selectivity of aromatics decreases above 425 °C. This result is consistent with the assumption that aromatic hydrocarbons play a role as intermediates in the kinetic reaction scheme; as conversion increases (in this case as a result of temperature increase), their concentration decreases in the reaction medium. However, the concentration of light olefins and also of C_{5+} hydrocarbons increases with temperature, although the latter to a lesser extent.

An analysis of the results in Figure 5 reveal that an increase in temperature reduces the apparent deactivation. These results

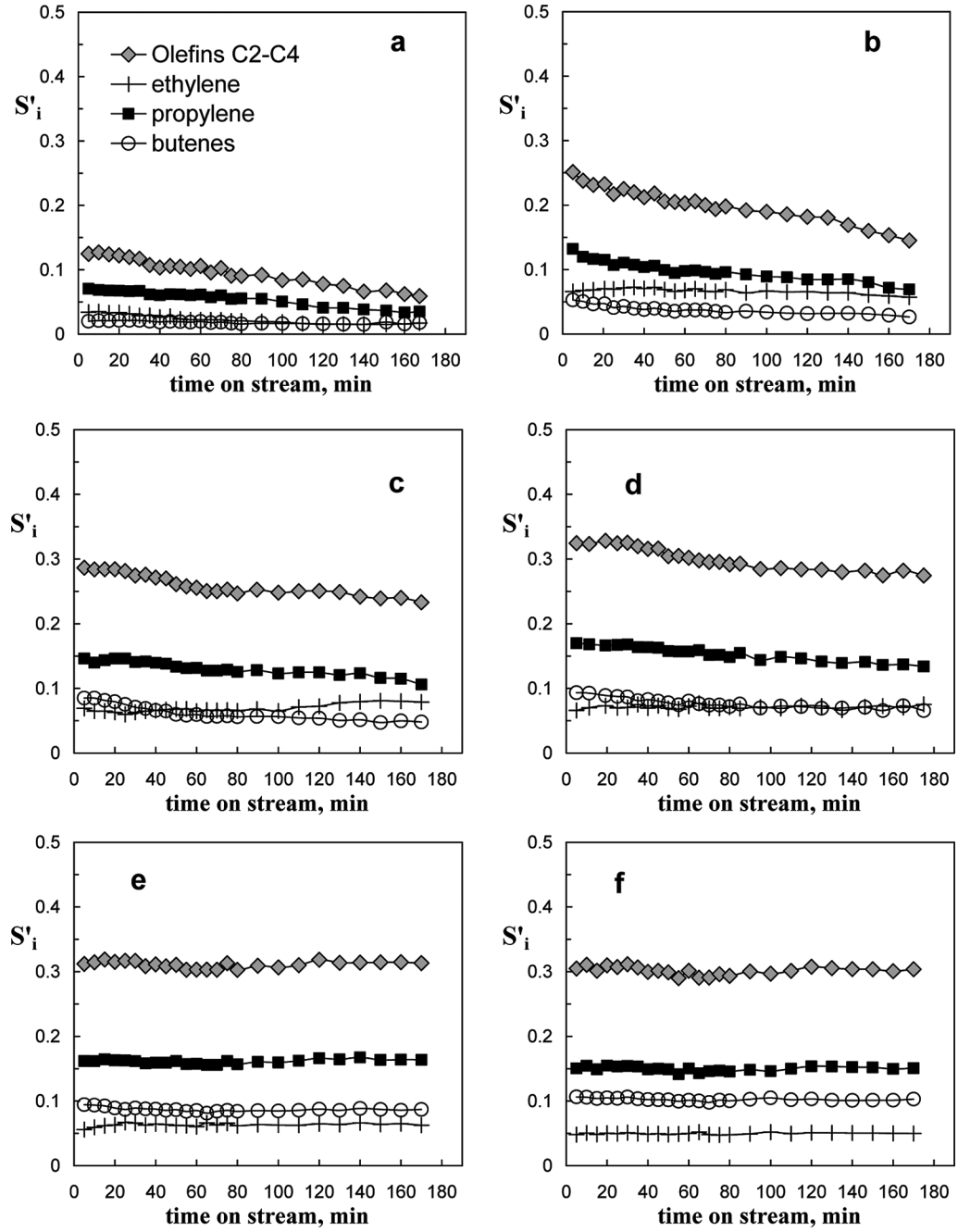

Figure 3. Effect of methanol content in the feed on the evolution with time on stream of the selectivity of olefins and to each individual olefin. Operating conditions: 450 °C; space time, 0.371 (g of catalyst) h (g of oxygenates)$^{-1}$. (a) Feed, crude bio-oil; (b) bio-oil/methanol, 4:1 mass ratio; (c) bio-oil/methanol, 3:2 mass ratio; (d) bio-oil/methanol, 1:1 mass ratio; (e) bio-oil/methanol, 2:3 mass ratio; (f) methanol.

are consistent with the aforementioned autocatalytic nature of deactivation, which is dependent on oxygenate concentration.

Figure 7 shows the TPO combustion curves of the coke deposited at different reaction temperatures. The values of total coke content and of thermal and catalytic fraction contents are listed in Table 3 (5% maximum relative error). Total coke content has a maximum value (5.84 wt %) at an intermediate temperature (425 °C) due to the opposite effect of temperature on the thermal and catalytic coke contents, which is explained by the aforementioned effect of oxygenate content in the reaction medium on the deposition of the two types of coke. Thus, thermal coke content increases as temperature is increased to 450 °C. Nevertheless, thermal coke content is lower at 500 °C, given that the concentration of the precursor for this type of coke (bio-oil) is lower in the reaction medium due to its high conversion at this temperature. Catalytic coke progressively decreases as conversion increases (oxygenate concentration decreases in the reaction medium) by increasing temperature in the 400−500 °C range.

Figure 8 shows the effect of temperature on the evolution with time on stream of the selectivities corresponding to the lump of olefins and to each individual olefin. At low temperature (400 °C) the selectivity of ethylene is similar to that of propylene, and both are almost twice that of butenes. As temperature is increased, ethylene selectivity is almost constant, whereas the selectivities of propylene and butenes steadily increase. The selectivity of butenes at 500 °C is slightly higher than that of ethylene, and propylene selectivity is twice that of ethylene and butenes. There is a slight decrease in the selectivity of olefins with time on stream, which has a similar effect on each individual olefin.

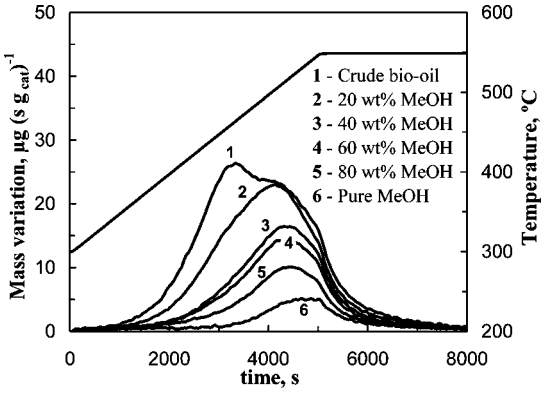

Figure 4. Effect of methanol content in the feed on the TPO combustion curve of the coke deposited on the catalyst. Operating conditions: 450 °C; space time, 0.371 (g of catalyst) h (g of oxygenates)$^{-1}$.

Table 2. Effect of Methanol Content in the Feed on the Total Coke Content (C_{cT}), Thermal Coke Fraction (f_{c1}), and Coke Content of Thermal Origin (C_{c1}) and Catalytic Origin (C_{c2})[a]

feed	C_{CT} (wt %)	f_{C1}	C_{C1} (wt %)	C_{C2} (wt %)
crude bio-oil	7.31	0.185	1.35	5.95
80:20 bio-oil/MeOH	5.66	0.140	0.79	4.86
60:40 bio-oil/MeOH	3.64	0.114	0.41	3.22
50:50 bio-oil/MeOH	3.13	0.098	0.31	2.83
40:60 bio-oil/MeOH	2.18	0.055	0.12	2.06
pure MeOH	0.88			0.88

[a] Operating conditions: 450 °C, space time, 0.371 (g of catalyst) h (g of oxygenates)$^{-1}$.

3.3. Effect of Space Time. Figure 9 shows the results of the evolution with time on stream of product yields and oxygenates concentration at the reactor outlet. Each graph corresponds to a space time value, while the other conditions are the same. The results correspond to a bio-oil/methanol feed with 50 wt % of bio-oil, given that this composition allows obtaining the aforementioned good results. Temperature, 500 °C, is suitable for maximizing the selectivity of C_2-C_4 olefins because higher temperatures cause hydrothermal stability problems in the catalyst when used in reaction-regeneration cycles.

Figure 10 shows the effect of space time on the conversion of bio-oil in the mixture at zero time on stream. There is a progressive increase in the conversion by increasing space time, whereby at 500 °C and with a space time of 0.37 (g of catalyst) h (g of oxygenates) $^{-1}$ 94 wt % initial conversion of the bio-oil in the feed is achieved.

Space time also has a significant effect on product selectivity at zero time on stream (Figure 10). Olefin selectivity increases slightly with an increase in space time, similarly to light paraffin selectivity, reaching 48 wt % of C_2-C_4 olefins at 0.37 (g of catalyst) h (g of oxygenates)$^{-1}$, of which 50 wt % is propene. The selectivity of aromatics hardly changes, whereas that to nonaromatic C_{5+} hydrocarbons progressively decreases.

It is noteworthy that the apparent deactivation of the catalyst significantly attenuates when increasing space time (Figure 9), which is consistent with the aforementioned hypothesis that oxygenates contained in the feed are the main precursors of coke deposition. This hypothesis also holds true in the results. The results in Figure 11, showing the TPO curves for the combustion of the coke deposited on the deactivated catalysts in runs with different space time, are also consistent with this hypothesis. As observed, an increase in space time reduces total coke content, which is due to the decrease in the thermal and catalytic origin fractions (Table 4, in which the maximum relative error of the results is 5%).

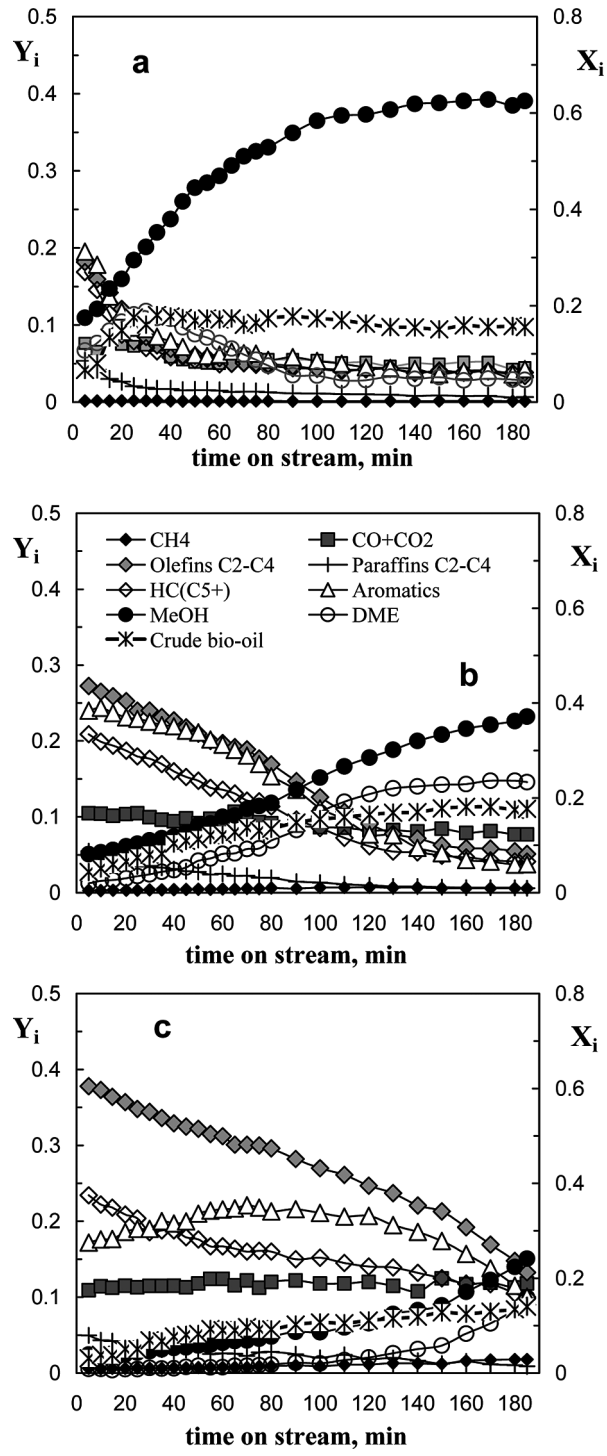

Figure 5. Effect of reaction temperature on the evolution with time on stream of product yields and oxygenate concentration at the reactor outlet. Operating conditions: Feed, mixture bio-oil/methanol of 50 wt %; space time, 0.243 (g of catalyst) h (g of oxygenates)$^{-1}$; (a) 400, (b) 450, and (c) 500 °C.

The previous results are consistent with the kinetic scheme in Figure 12, which may be taken as the basis for subsequent kinetic studies in which the rate of lump interconversion is quantified. Line thickness is related to the significance of the steps. The main peculiarity compared to the transformation of methanol in this temperature range (which must be attributed to bio-oil in the feed) is the direct formation of aromatics, C_{5+} hydrocarbons, and CO + CO_2. The formation of thermal coke takes place exclusively from the bio-oil fed, whereas the formation of thermal coke occurs mainly from the degradation

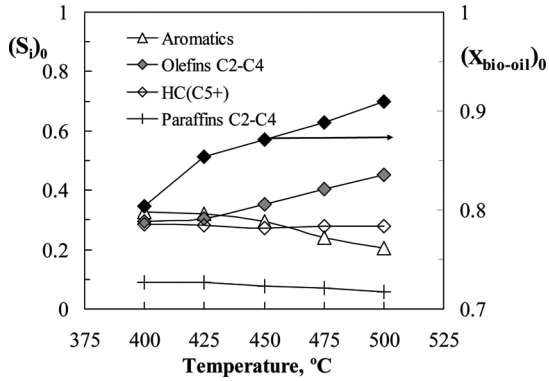

Figure 6. Effect of reaction temperature on bio-oil conversion and on the selectivity of hydrocarbon product lumps at zero time on stream. Operating conditions: Feed, 50 wt % bio-oil/methanol mixture; space time, 0.243 (g of catalyst) h (g of oxygenates)$^{-1}$.

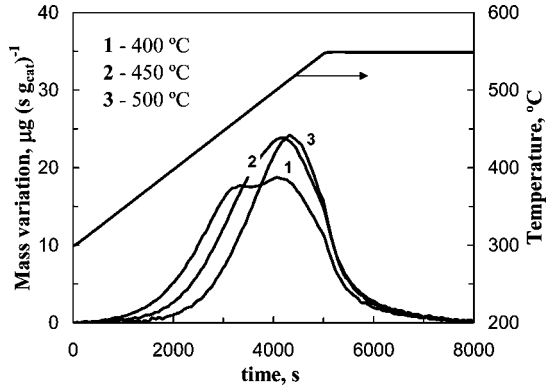

Figure 7. Effect of reaction temperature on the TPO combustion curve of the coke deposited on the catalyst. Operating conditions: Feed, 50 wt % bio-oil/methanol mixture; space time, 0.243 (g of catalyst) h (g of oxygenates)$^{-1}$.

Table 3. Values of Total Coke Content (C_{cT}), Thermal Coke Fraction (f_{c1}), and Coke Content of Thermal Origin (C_{c1}) and Catalytic Origin (C_{c2}) for Different Reaction Temperatures[a]

temperature, °C	C_{CT} (wt %)	f_{C1}	C_{C1} (wt %)	C_{C2} (wt %)
400	5.38	0.107	0.57	4.81
425	5.84	0.272	1.59	4.25
450	5.72	0.306	1.75	3.97
500	4.72	0.328	1.55	3.17

[a] Operating conditions: Feed, 50 wt % bio-oil/methanol mixture; space time, 0.243 (g of catalyst) h (g of oxygenates)$^{-1}$.

of bio-oil and methanol, which are more influential steps than those involving hydrocarbon compounds (mainly aromatics).

Conclusions

Conversion of the bio-oil in the bio-oil/methanol mixture peaks for a methanol content of about 50 wt %, with a significant decrease in CO and CO_2 yields compared to that occurring when transforming crude bio-oil. For higher contents, the adsorbed methanol saturates the acid sites, lowering the conversion of bio-oil oxygenates.

By increasing methanol content in the feed there is a progressive and pronounced decrease in the initial yield of aromatic hydrocarbons, the yields of light paraffins and C_{5+} steadily increase, and the initial yield of olefins increases asymptotically up to 30 wt %. Propylene is always the predominant olefin, and the proportion of ethylene in the olefin lump significantly decreases by increasing methanol content,

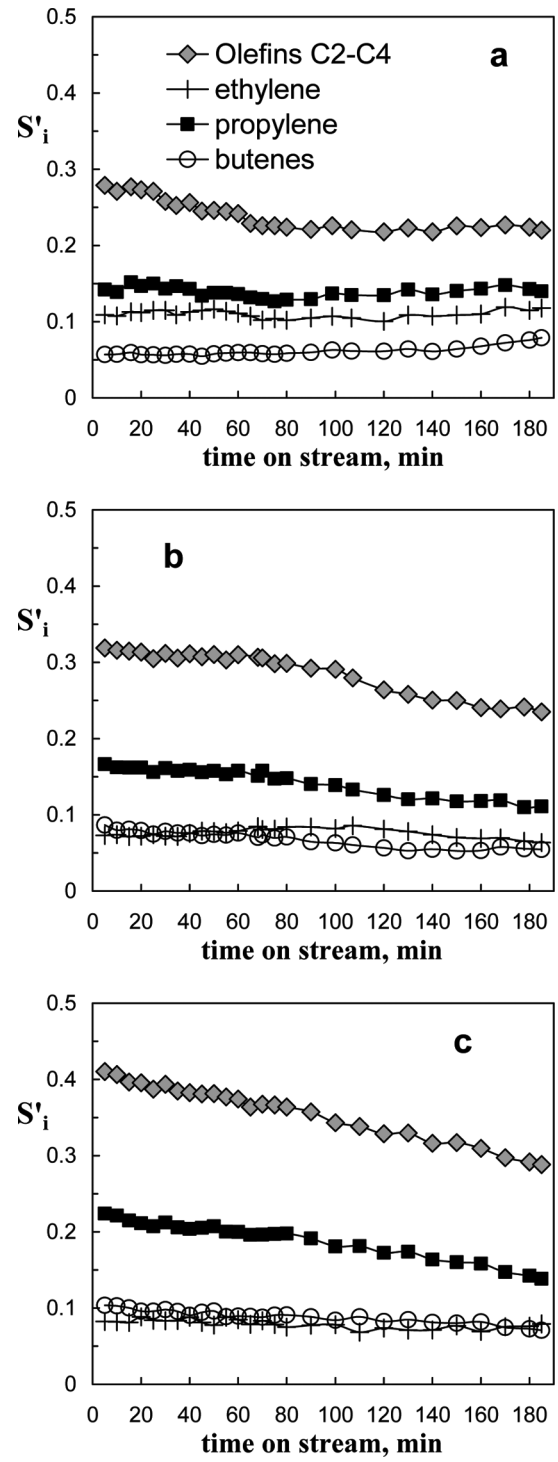

Figure 8. Effect of reaction temperature on the evolution with time on stream of the selectivity of olefins and to each individual olefin. Operating conditions: Feed, 50 wt % bio-oil/methanol mixture; space time, 0.243 (g of catalyst) h (g of oxygenates)$^{-1}$; (a) 400, (b) 450, (c) 500 °C.

whereas that of butenes increases. Methanol in the feed is effective for reducing catalyst deactivation, as it attenuates the deposition of pyrolytic lignin and, to a lesser extent, the deposition of catalytic origin coke.

The conversion of bio-oil and the selectivity of light olefins increase with temperature. The selectivity of C_{5+} hydrocarbons changes slightly, passing through a slight minimum, whereas the selectivity of aromatics peaks between 425 and 450 °C.

Bio-oil conversion increases with space time, so that at 500 °C and with a space time of 0.37 (g of catalyst) h (g of

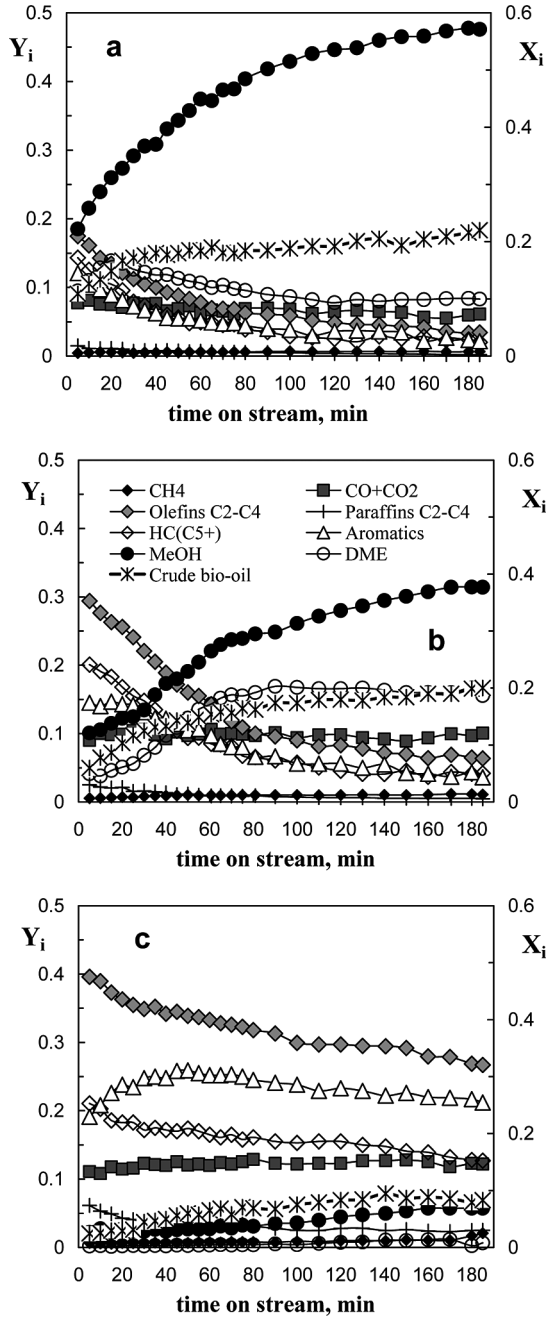

Figure 9. Effect of space time on the evolution with time on stream of product yields and oxygenate concentration at the reactor outlet. Operating conditions: Feed, 50 wt % bio-oil/methanol mixture; 500 °C; (a) 0.060, (b) 0.121, and (c) 0.371 (g of catalyst) h (g of oxygenates)$^{-1}$.

oxygenates)$^{-1}$ a bio-oil conversion of 94 wt % is achieved at zero time on stream. Olefin selectivity increases slightly with space time, similarly to light paraffin selectivity. The selectivity of aromatics does not change, whereas that of nonaromatic C_{5+} hydrocarbons progressively decreases.

The progressive decrease in deactivation with increasing temperature and space time is explained by the prevailing effect of bio-oil oxygenate concentration in the reaction medium.

These results are relevant as a starting point for studies on the incorporation of crude bio-oil together with methanol in the MTO process. There is a growing implementation of this process using natural gas as feedstock for the synthesis of methanol. The integration of these feedstocks would involve the use of

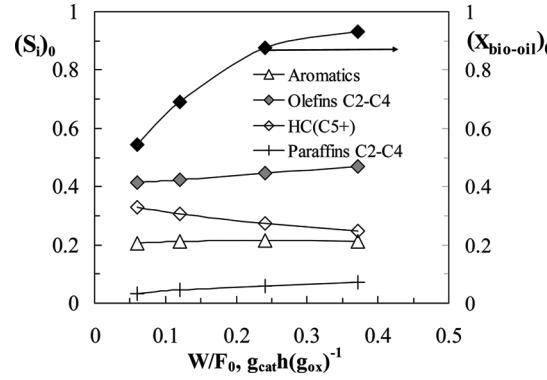

Figure 10. Effect of space time on bio-oil conversion and on the selectivity of hydrocarbon product lumps at zero time on stream. Operating conditions: Feed, 50 wt % bio-oil/methanol mixture; 500 °C.

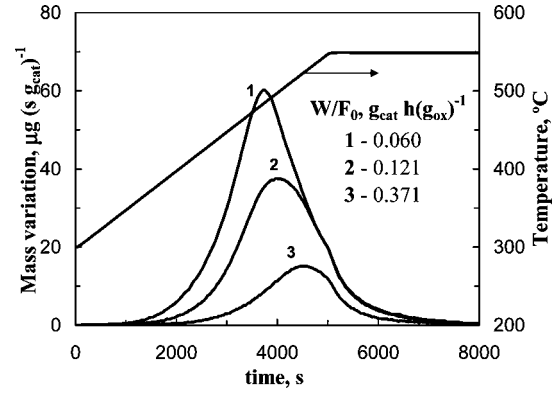

Figure 11. Effect of space time on the TPO combustion curve of the coke deposited on the catalyst. Operating conditions: Feed, 50 wt % bio-oil/methanol mixture; 500 °C.

Table 4. Values of Total Coke Content (C_{cT}), Thermal Coke Fraction (f_{c1}), and Coke Content of Thermal Origin (C_{c1}) and Catalytic Origin (C_{c2}) for Different Values of Space Time[a]

W/F_o, $g_{catalyst}$ h $(g_{oxygenates})^{-1}$	C_{CT} (wt %)	f_{C1}	C_{C1} (wt %)	C_{C2} (wt %)
0.060	11.58	0.452	5.23	6.35
0.121	7.92	0.369	2.93	4.99
0.243	4.72	0.328	1.55	3.17
0.371	2.97	0.302	0.90	2.07

[a] Operating conditions: Feed, 50 wt % bio-oil/methanol mixture; 500 °C.

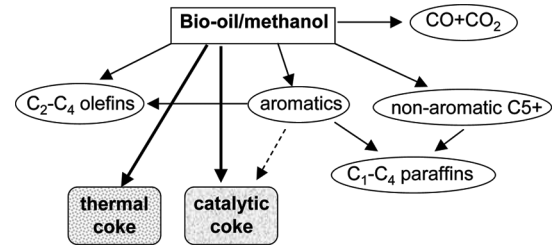

Figure 12. Kinetic scheme for the transformation of the bio-oil/methanol mixture into hydrocarbons on HZ-80 zeolite in the 400−500 °C range.

natural gas and biomass as alternative sources to petroleum for obtaining olefins, other chemicals, and fuels.

Acknowledgment

This work was carried out with the financial support of the Department of Education, Universities and Research of the Basque Government (Project GIC07/24-IT-220-07) and

of the Ministry of Science and Innovation of the Spanish Government (Project CTQ2006-12006/PPQ).

Nomenclature

C_{ci} = content of i coke fraction in the catalyst ($i = 1$, thermal coke; $i = 2$, catalytic coke)
d_p = pore diameter, Å
F_0 = mass flow of oxygenates (in bio-oil and methanol) fed into the reactor, g h^{-1}
f_{c1} = mass fraction of thermal origin coke in the catalyst
$(m_{bio\text{-}oil})_i$, $(m_{bio\text{-}oil})_o$ = mass flow of bio-oil at the reactor inlet and outlet, g h^{-1}
S_{BET} = BET specific surface, m^2 g^{-1}
S_i = selectivity of product lump i, by mass unit of product amount excluding CO and CO_2
S_i' = selectivity of product lump i, by mass unit of total product amount
T = temperature, °C
t = time on stream, h
V_p = pore volume, cm^3 g^{-1}
W = mass of catalyst, g
X_i = lump i concentration, mass fraction on a water-free basis
$X_{bio\text{-}oil}$ = bio-oil conversion
Y_i = yield of product lump i

Literature Cited

(1) Huber, G. W.; Iborra, S.; Corma, A. Synthesis of transportation fuels from biomass: Chemistry, catalysts, and engineering. *Chem. Rev.* **2006**, *106*, 4044–4098.

(2) Stöcker, M. Biofuels and biomass-to-liquid fuels in the biorefinery: Catalytic conversion of lignocellulosic biomass using porous materials. *Angew. Chem., Int. Ed.* **2008**, *48*, 9200–9211.

(3) Mohan, D.; Pittman, C. U.; Steele, P. H. Pyrolysis of wood/biomass for bio-oil: A critical review. *Energy Fuels* **2006**, *20*, 848–889.

(4) Huber, G. W.; Corma, A. Synergies between bio- and oil refineries for the production of fuels from biomass. *Angew. Chem., Int. Ed.* **2007**, *46*, 7184–7201.

(5) Corma, A.; Huber, G. W.; Sauvanaud, L.; O'Connor, P. Processing biomass-derived oxygenates in the oil refinery: Catalytic cracking (FCC) reaction pathways and role of catalyst. *J. Catal.* **2007**, *247*, 307–327.

(6) Domine, M. E.; van Veen, A. C.; Schuurman, Y.; Mirodatos, C. Coprocessing of oxygenated biomass compounds and hydrocarbons for the production of sustainable fuel. *ChemSusChem* **2008**, *1*, 179–181.

(7) Atutxa, A.; Aguado, R.; Gayubo, A. G.; Olazar, M.; Bilbao, J. Kinetic description of catalytic pyrolysis of biomass in a conical spouted bed reactor. *Energy Fuels* **2005**, *19*, 765–774.

(8) Aho, A.; Kumar, N.; Eränen, K.; Salmi, T.; Hupa, M.; Murzin, D. Y. Catalytic pyrolysis of woody biomass in a fluidized bed reactor: Influence of the zeolite structure. *Fuel* **2008**, *87*, 2493–2501.

(9) Horne, P. A.; Williams, P. T. Upgrading of biomass-derived pyrolytic vapours over zeolite ZSM-5 catalyst: Effect of catalyst dilution on product yields. *Fuel* **1995**, *75*, 1043–1050.

(10) Pütün, E.; Uzun, B. B., Pütün, A. E. Rapid pyrolysis of olive residue. 2. effect of catalytic upgrading of pyrolysis vapors in a two-stage fixed-bed reactor. *Energy Fuels*, in press.

(11) Aguado, R.; Olazar, M.; San José, M. J.; Aguirre, G.; Bilbao, J. Pyrolysis of sawdust in a conical spouted bed reactor. Yields and product composition. *Ind. Eng. Chem. Res.* **2000**, *39*, 1925–1933.

(12) Oasmaa, A.; Kuoppala, E.; Gust, S.; Solantausta, Y. Fast pyrolysis of forestry residue. 1. Effect of extractives on phase separation of pyrolysis liquids. *Energy Fuels* **2003**, *17*, 1–12.

(13) Oasmaa, A.; Kuoppala, E.; Solantausta, Y. Fast pyrolysis of forestry residue. 2. Physicochemical composition of product liquid. *Energy Fuels* **2003**, *17*, 433–443.

(14) Czernik, S.; Bridgwater, A. V. Overview of applications of biomass fast pyrolysis oil. *Energy Fuels* **2004**, *18*, 590–598.

(15) Gayubo, A. G.; Aguayo, A. T.; Atutxa, A.; Aguado, R.; Bilbao, J. Transformation of oxygenate components of biomass pyrolysis-oil on a HZSM-5 zeolite. I. Alcohols and phenols. *Ind. Eng. Chem. Res.* **2004**, *43*, 2610–2618.

(16) Gayubo, A. G.; Aguayo, A. T.; Atutxa, A.; Aguado, R.; Olazar, M.; Bilbao, J. Transformation of oxygenate components of biomass pyrolysis-oil on a HZSM-5 zeolite. II. Aldehydes, ketones and acids. *Ind. Eng. Chem. Res.* **2004**, *43*, 2619–2626.

(17) Basagiannis, A. C.; Verykios, X. E. Steam reforming of the aqueous fraction of bio-oil over structured $Ru/MgO/Al_2O_3$ catalysts. *Catal. Today* **2007**, *127*, 256–264.

(18) Bimbela, F.; Oliva, M.; Ruiz, J.; García, L.; Arauzo, J. Catalytic steam reforming of model compounds of biomass pyrolysis liquids in fixed bed: Acetol and n-butanol. *J. Anal. Appl. Pyrolysis* **2007**, *79*, 112–120.

(19) Ramos, M. C.; Navascués, A. I.; García, L.; Bilbao, R. Hydrogen production by catalytic steam reforming of acetol, a model compound of bio-oil. *Ind. Eng. Chem. Res.* **2007**, *46*, 2399–2406.

(20) Diebold, J. P.; Czernik, S. Additives to lower and stabilize the viscosity of pyrolysis oils during storage. *Energy Fuels* **1997**, *11*, 1081–1091.

(21) Oasmaa, A.; Kuoppala, E.; Selin, F. F.; Gust, S.; Solantausta, Y. Fast pyrolysis of forestry residue and pine. 4. Improvement of the product quality by solvent addition. *Energy Fuels* **2004**, *18*, 1578–1583.

(22) Gayubo, A. G.; Valle, B.; Aguayo, A. T.; Olazar, M.; Bilbao, J. Co-feeding methanol for enhancing the valorisation of crude bio-oil by catalytic transformation. *Energy Fuels* **2009**, *23*, 4129–4136.

(23) Gayubo, A. G.; Valle, B.; Aguayo, A. T.; Olazar, M.; Bilbao, J. Pyrolytic lignin removal to valorise biomass pyrolysis crude bio-oil by catalytic transformation. *J. Chem. Technol. Biotechnol.*, in press.

(24) Chang, C. D.; Silvestri, A. J. The conversion of methanol and other O-compounds to hydrocarbons over zeolite catalysts. *J. Catal.* **1977**, *47*, 249–259.

(25) Gayubo, A. G.; Benito, P. L.; Aguayo, A. T.; Olazar, M.; Bilbao, J. Relationship between surface acidity and activity of HZSM5 zeolite based catalysts in the transformation of methanol into hydrocarbons. *J. Chem. Tech. Biotechnol.* **1996**, *65*, 186–192.

(26) Olazar, M.; Aguado, R.; San José, M. J.; Bilbao, J. Kinetic study of fast pyrolysis of sawdust in a conical spouted bed reactor in the 400−500 °C range. *J. Chem. Tech. Biotechnol.* **2001**, *76*, 469–476.

(27) Aguayo, A. T.; Gayubo, A. G.; Ereña, J.; Olazar, M.; Arandes, J. M.; Bilbao, J. Isotherms of chemical adsorption of bases on solid catalysts for acidity measurement. *J. Chem. Tech. Biotechnol.* **1994**, *60*, 141–146.

(28) Benito, A. G.; Gayubo, A. G.; Aguayo, A. T.; Olazar, M.; Bilbao, J. Effect of Si/Al ratio and of acidity of H-ZSM5 zeolites on the primary products of methanol to gasoline conversion. *J. Chem. Tech. Biotechnol.* **1996**, *66*, 183–191.

(29) Ortega, J.; Gayubo, A. G.; Aguayo, A. T.; Benito, P. L.; Bilbao, J. Role of coke characteristics in the regeneration of a catalyst for the MTG process. *Ind. Eng. Chem. Res.* **1997**, *36*, 60–66.

(30) Dao, L. H.; Haniff, M.; Houle, A.; Lamothe, D. Reactions of model compounds of biomass-pyrolysis oils over ZSM-5 zeolite. *ACS Symp. Ser.* **1988**, *376*, 328–341.

(31) Dahl, I. M.; Kolboe, S. On the reaction-mechanism for hydrocarbon formation from methanol over SAPO-34. 1. Isotopic labelling studies of the co-reaction of ethene and methanol. *J. Catal.* **1994**, *149*, 458–464.

(32) Mikkelsen, O.; Ronning, P. O.; Kolboe, S. Use of isotopic labeling for mechanistic studies of the methanol-to-hydrcarbons reaction. Methylation of toluene with methanol over HZSM-5, H-mordenite and H-beta. *Microporous Mesoporous Mater.* **2000**, *40*, 95–113.

(33) Wang, W.; Jiang, Y.; Hunger, M. Mechanistic Investigations of the methanol-to-olefin (MTO) process on acidic zeolite catalysts by in situ solid-state NMR spectroscopy. *Catal. Today* **2006**, *113*, 102–114.

(34) Guisnet, M.; Magnoux, P. Organic chemistry of coke formation. *Appl. Catal., A* **2001**, *212*, 83–96.

(35) Cerqueira, H. S.; Caeiro, G.; Costa, L.; Ramôa Ribeiro, F. Deactivation of FCC catalysts. *J. Mol. Catal. A: Chem.* **2008**, *292*, 1–13.

(36) Aguayo, A. T.; Gayubo, A. G.; Vivanco, R.; Alonso, A.; Bilbao, J. Initiation step and reactive intermediates in the transformation of methanol into olefins over SAPO-18 catalyst. *Ind. Eng. Chem. Res.* **2005**, *44*, 7279–7286.

(37) Gayubo, A. T.; Aguayo, A. T.; Atutxa, A.; Valle, B.; Bilbao J. Undesired components in the transformation of biomass pyrolysis-oil into hydrocarbons on a HZSM-5 zeolite. *J. Chem. Tech. Biotechnol.* **2005**, *80*, 1244–1251.

(38) Arandes, J. M.; Abajo, I.; Fernández, I.; Azkoiti, M. J.; Bilbao, J. Effect of HZSM-5 zeolite addition to a FCC catalyst. Study in a laboratory reactor operating under industrial conditions. *Ind. Eng. Chem. Res.* **2000**, *39*, 1917–1924.

Received for review July 30, 2009
Revised manuscript received October 9, 2009
Accepted November 2, 2009

IE901204N